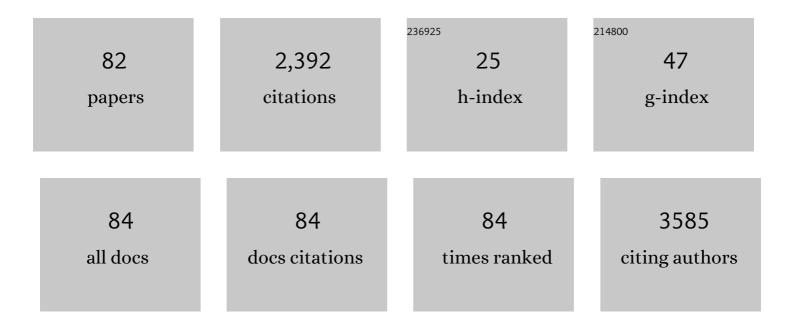
Yuanyuan Zhang

List of Publications by Year in descending order

Source: https://exaly.com/author-pdf/4198900/publications.pdf Version: 2024-02-01



#	Article	IF	CITATIONS
1	Synthesizing Superior Flexible Oxide Perovskite Ceramic Nanofibers by Precisely Controlling Crystal Nucleation and Growth. Small, 2022, 18, e2106500.	10.0	16
2	Co3O4 Nanoparticles Uniformly Dispersed in Rational Porous Carbon Nano-Boxes for Significantly Enhanced Electrocatalytic Detection of H2O2 Released from Living Cells. International Journal of Molecular Sciences, 2022, 23, 3799.	4.1	7
3	Fabrication of Flexible Mesoporous Black Nb ₂ O ₅ Nanofiber Films for Visibleâ€Lightâ€Driven Photocatalytic CO ₂ Reduction into CH ₄ . Advanced Materials, 2022, 34, e2200756.	21.0	104
4	Spatial enhancement due to statistical learning tracks the estimated spatial probability. Attention, Perception, and Psychophysics, 2022, , .	1.3	3
5	Dynamic 3D DNA Rolling Walkers via Directional Movement on a Lipid Bilayer Supported by Au@Fe ₃ O ₄ Nanoparticles for Sensitive Detection of MiRNA-16. Analytical Chemistry, 2022, 94, 8346-8353.	6.5	14
6	Isolation, Antibacterial, Nematicidal and Anxiolytic Activities of Essential Oil from <i>Cinnamomum longepaniculatum</i> (Gamble) N. Chao ex H. W. Li Leaves. Journal of Essential Oil-bearing Plants: JEOP, 2022, 25, 581-600.	1.9	3
7	Disruption of Epithelial Barrier of Caco-2 Cell Monolayers by Excretory Secretory Products of Trichinella spiralis Might Be Related to Serine Protease. Frontiers in Microbiology, 2021, 12, 634185.	3.5	13
8	Dielectric Relaxation Behavior of BTO/LSMO Heterojunction. Nanomaterials, 2021, 11, 1109.	4.1	3
9	Structural, electrical, magnetic and optical properties of BaTi1â^'x(Ni1/2Nb1/2)xO3 ceramics. Journal of Materials Science: Materials in Electronics, 2021, 32, 19519-19528.	2.2	1
10	Bifunctional Moderator-Powered Ratiometric Electrochemiluminescence Enzymatic Biosensors for Detecting Organophosphorus Pesticides Based on Dual-Signal Combined Nanoprobes. Analytical Chemistry, 2021, 93, 8783-8790.	6.5	41
11	Specific cation stoichiometry control of SrMnO3-δ thin films via RHEED oscillations. Applied Physics Letters, 2021, 118, .	3.3	2
12	Ultrasensitive Detection of Amyloid β Oligomers Based on the "DD–A―FRET Binary Probes and Quadrivalent Cruciform DNA Nanostructure-Mediated Cascaded Amplifier. ACS Applied Materials & Interfaces, 2021, 13, 32013-32021.	8.0	13
13	Oxygenâ€vacancyâ€enhanced Catalytic Activity of Au@Co ₃ O ₄ /CeO ₂ Yolkâ€shell Nanocomposite to Electrochemically Detect Hydrogen Peroxide. Electroanalysis, 2021, 33, 2180-2186.	2.9	4
14	Enhancement of Energy-Storage Density in PZT/PZO-Based Multilayer Ferroelectric Thin Films. Nanomaterials, 2021, 11, 2141.	4.1	17
15	Cenozoic Crustallyâ€derived Carbonateâ€rich Magmatic Rocks in West Junggar, North Xinjiang, Western China: Geochronology, Geochemistry and Tectonic Implications. Acta Geologica Sinica, 2021, 95, 1112-1127.	1.4	0
16	The effect of stress on the magnetic properties of sol–gel-derived Pr0.9Ca0.1MnO3 thin films. Journal of Materials Science: Materials in Electronics, 2021, 32, 23126-23133.	2.2	0
17	Superior Flexibility in Oxide Ceramic Crystal Nanofibers. Advanced Materials, 2021, 33, e2105011.	21.0	46
18	Effect of polarization on photoexcited carrier dynamics in ferroelectric thin films. Journal of the European Ceramic Society, 2021, 41, 151-157.	5.7	1

#	Article	IF	CITATIONS
19	High-Performance Photodetectors with an Ultrahigh Photoswitching Ratio and a Very Fast Response Speed in Self-Powered Cu ₂ ZnSnS ₄ /CdS PN Heterojunctions. ACS Applied Electronic Materials, 2021, 3, 4135-4143.	4.3	10
20	Autophagy Induced by Palmitic Acid Regulates Neutrophil Adhesion Through the Granule-Dependent Degradation of αMβ2 Integrin in Dairy Cows With Fatty Liver. Frontiers in Immunology, 2021, 12, 726829.	4.8	2
21	Nanometer-Thick Metastable Zinc Blende Î ³ -MnTe Single-Crystalline Films for High-Performance Ultraviolet and Broadband Photodetectors. ACS Applied Nano Materials, 2020, 3, 12046-12054.	5.0	8
22	Fe doping effect on the structural, ferroelectric and magnetic properties of polycrystalline BaTi1â^'xFexO3 ceramics. Journal of Materials Science: Materials in Electronics, 2020, 31, 14487-14493.	2.2	7
23	Acceleration of goethite-catalyzed Fenton-like oxidation of ofloxacin by biochar. Journal of Hazardous Materials, 2020, 397, 122783.	12.4	71
24	Effect of recombinant serine protease from adult stage of Trichinella spiralis on TNBS-induced experimental colitis in mice. International Immunopharmacology, 2020, 86, 106699.	3.8	18
25	Ni doping effect on the magnetic properties of polycrystalline Y-type hexaferrite Ba0.5Sr1.5Zn2Fe12â^'xNixO22. Journal of Materials Science: Materials in Electronics, 2020, 31, 6538-6546.	2.2	2
26	Extracellular Vesicles Derived From Trichinella spiralis Muscle Larvae Ameliorate TNBS-Induced Colitis in Mice. Frontiers in Immunology, 2020, 11, 1174.	4.8	44
27	Spinâ€phonon coupling and twoâ€magnons scattering behaviors in hexagonal NiAsâ€type antiferromagnetic MnTe epitaxial films. Journal of Raman Spectroscopy, 2020, 51, 1383-1389.	2.5	10
28	Correlation of oxygen vacancy and Jahn–Teller polarons in epitaxial perovskite SrMnO3 ultrathin films: Dielectric spectroscopy investigations. Applied Physics Letters, 2020, 116, .	3.3	5
29	Revealing a metastable cubic phase in CoFe2O4–SrTiO3 three-dimensional network heteroepitaxial nanostructure. Journal of Applied Physics, 2020, 128, 225303.	2.5	0
30	A Novel Catalystâ€Free Synthesis of 2,2â€Diaryl Enamides from Stilbenes via a Nitrene Transfer Reaction. European Journal of Organic Chemistry, 2019, 2019, 5720-5724.	2.4	6
31	Room temperature hidden state in a manganite observed by time-resolved X-ray diffraction. Npj Quantum Materials, 2019, 4, .	5.2	2
32	Polymer Template Synthesis of Soft, Light, and Robust Oxide Ceramic Films. IScience, 2019, 15, 185-195.	4.1	34
33	Polyelectrolyte nanocapsule probe for the determination of imidacloprid in agricultural food samples. Food and Agricultural Immunology, 2019, 30, 432-445.	1.4	9
34	Magnetism tuned by intercalation of various metal ions in coordination polymer. Chinese Chemical Letters, 2019, 30, 1390-1392.	9.0	15
35	Shape-Controlled Synthesis of Trimetallic PtPdCu Nanocrystals and Their Electrocatalytic Properties. ACS Applied Energy Materials, 2019, 2, 2515-2523.	5.1	27
36	Temperatureâ€Dependent Spin–Orbit Torques in Perpendicular Magnetic [Co/Ni] N /TbCo Composite Films. Advanced Electronic Materials, 2019, 5, 1900014.	5.1	7

#	Article	IF	CITATIONS
37	PtFeCu Concave Octahedron Nanocrystals as Electrocatalysts for the Methanol Oxidation Reaction. Langmuir, 2019, 35, 16752-16760.	3.5	24
38	Microstructure evolution and strengthening mechanism of Cu <i>_x</i> [Ni ₃ Mo] alloys. Materials Science and Technology, 2019, 35, 98-106.	1.6	2
39	Fast Ion Transport Pathway Provided by Polyethylene Glycol Confined in Covalent Organic Frameworks. Journal of the American Chemical Society, 2019, 141, 1923-1927.	13.7	217
40	Metallic few-layered VSe ₂ nanosheets: high two-dimensional conductivity for flexible in-plane solid-state supercapacitors. Journal of Materials Chemistry A, 2018, 6, 8299-8306.	10.3	89
41	Microstructure evolution determined by the crystalline phases competition in self-assembled WO3-BiVO4 hetero nanostructures. Journal of Applied Physics, 2018, 123, 085305.	2.5	4
42	Trimetallic PtPdCu nanowires as an electrocatalyst for methanol and formic acid oxidation. New Journal of Chemistry, 2018, 42, 19083-19089.	2.8	35
43	Facile Synthesis of Fe3Pt-Ag Nanocomposites for Catalytic Reduction of Methyl Orange. Chemical Research in Chinese Universities, 2018, 34, 871-876.	2.6	13
44	The effect of film/electrode interfaces on the dielectric responses of highly (000 <i>l</i>)-oriented M-type BaFe12O19 thin films synthesized using chemical solution deposition. Applied Physics Letters, 2018, 113, .	3.3	5
45	Synthesis and evaluation of a novel water-soluble high Se-enriched Astragalus polysaccharide nanoparticles. International Journal of Biological Macromolecules, 2018, 118, 1438-1448.	7.5	30
46	Hierarchical NiCo ₂ O ₄ @NiCo ₂ S ₄ Nanocomposite on Ni Foam as an Electrode for Hybrid Supercapacitors. ACS Omega, 2018, 3, 5634-5642.	3.5	99
47	A Flexible Metal–Organic Framework with 4-Connected Zr ₆ Nodes. Journal of the American Chemical Society, 2018, 140, 11179-11183.	13.7	158
48	Coral-Shaped MoS ₂ Decorated with Graphene Quantum Dots Performing as a Highly Active Electrocatalyst for Hydrogen Evolution Reaction. ACS Applied Materials & Interfaces, 2017, 9, 3653-3660.	8.0	98
49	The preparation, and structural and multiferroic properties of B-site ordered double-perovskite Bi ₂ FeMnO ₆ . Journal of Materials Chemistry C, 2017, 5, 5494-5500.	5.5	28
50	Thickness dependent magnetic properties of epitaxial La 0.7 Sr 0.3 MnO 3 thin films prepared by chemical solution deposition method. Ceramics International, 2017, 43, S493-S496.	4.8	3
51	Structure influence on the magnetic properties of La 0.7 Sr 0.3 MnO 3 /La 0.7 Ca 0.3 MnO 3 multilayer thin films fabricated by chemical solution deposition method. Ceramics International, 2017, 43, S497-S500.	4.8	2
52	Electric field control of magnetism in nickel with coaxial cylinder structure at room temperature by electric double layer gating. Journal of Materials Chemistry C, 2017, 5, 10609-10614.	5.5	3
53	Structural and magnetic properties of perovskite SrMnO 3 thin films grown by molecular beam epitaxy. Thin Solid Films, 2017, 644, 57-64.	1.8	14
54	Scaling behavior for (Bi0.5Na0.5)TiO3 based lead-free relaxor ferroelectric ceramics. Journal of Applied Physics, 2017, 122, .	2.5	25

YUANYUAN ZHANG

#	Article	IF	CITATIONS
55	Strong influence of polaron-polaron interaction on the magnetoresistance effect in La0.7A0.3MnO3 thin films. Applied Physics Letters, 2017, 111, 192408.	3.3	6
56	Threeâ€Dimensional Anionic Cyclodextrinâ€Based Covalent Organic Frameworks. Angewandte Chemie - International Edition, 2017, 56, 16313-16317.	13.8	290
57	Threeâ€Dimensional Anionic Cyclodextrinâ€Based Covalent Organic Frameworks. Angewandte Chemie, 2017, 129, 16531-16535.	2.0	54
58	Role of indium tin oxide electrode on the microstructure of self-assembled WO3-BiVO4 hetero nanostructures. Journal of Applied Physics, 2017, 122, .	2.5	6
59	Synthesis, Structure and Properties of Formamidineâ€ŧemplated Metal Formate Crystals. Crystal Research and Technology, 2017, 52, 1700195.	1.3	3
60	REGÎ ³ Contributes to Regulation of Hemoglobin and HemoglobinδSubunit. Oxidative Medicine and Cellular Longevity, 2017, 2017, 1-11.	4.0	7
61	Improved Performance of <scp>YIG</scp> (Y ₃ Fe ₅ O ₁₂) Films Grown on Ptâ€Buffered Si Substrates by Chemical Solution Deposition Technique. Journal of the American Ceramic Society, 2016, 99, 2217-2220.	3.8	8
62	Effect of Nb and more Fe ions co-doping on the microstructures, magnetic, and piezoelectric properties of Aurivillius Bi5Ti3FeO15 phases. Journal of Applied Physics, 2016, 120, .	2.5	19
63	Spinâ€glass state induced low field magnetizationâ€step effect in a Hg _{1â^'<i>x</i>} Mn _{<i>x</i>} Te single crystal. Physica Status Solidi (B): Basic Research, 2016, 253, 2015-2019.	1.5	0
64	Dielectric behaviors of Aurivillius Bi5Ti3Fe0.5Cr0.5O15 multiferroic polycrystals: Determining the intrinsic magnetoelectric responses by impedance spectroscopy. Scientific Reports, 2016, 5, 17846.	3.3	49
65	Iron oxyhydroxide nanorods with high electrochemical reactivity as a sensitive and rapid determination platform for 4-chlorophenol. Journal of Hazardous Materials, 2016, 307, 36-42.	12.4	12
66	Annealing Effect on the Physical Properties of La0.7Sr0.3MnO3Thin Films Grown on Si Substrates Prepared by Chemical Solution Deposition Method. Ferroelectrics, 2016, 491, 143-148.	0.6	0
67	Hollow Structured Micro/Nano MoS ₂ Spheres for High Electrocatalytic Activity Hydrogen Evolution Reaction. ACS Applied Materials & Interfaces, 2016, 8, 5517-5525.	8.0	190
68	Large room-temperature magnetoresistance in epitaxial La0.7Ca0.25Sr0.05MnO3 thin films prepared by sol–gel method. Journal of Sol-Gel Science and Technology, 2016, 78, 576-581.	2.4	10
69	Highly orientated growth and characterization of La0.7Sr0.3MnO3 thin films with different orientations on SrTiO3 substrates by chemical solution deposition method. Journal of Applied Physics, 2015, 117, 17E102.	2.5	8
70	Eicosapentaenoic acid (EPA) induced apoptosis in HepG2 cells through ROS–Ca2+–JNK mitochondrial pathways. Biochemical and Biophysical Research Communications, 2015, 456, 926-932.	2.1	40
71	Anti-inflammatory Activity and Mechanism of Surfactin in Lipopolysaccharide-Activated Macrophages. Inflammation, 2015, 38, 756-764.	3.8	68
72	Oxidative challenge enhances REGγ–proteasome-dependent protein degradation. Free Radical Biology and Medicine, 2015, 82, 42-49.	2.9	11

YUANYUAN ZHANG

#	Article	IF	CITATIONS
73	Structure, magnetic and transport properties of La0.7Ca0.3â^'Sr MnO3 thin films by sol–gel method. Ceramics International, 2015, 41, S381-S386.	4.8	60
74	Magnetic and Dielectric Properties in Multiferroic Y-type Hexaferrite. Molecular Crystals and Liquid Crystals, 2014, 603, 235-239.	0.9	6
75	Magnetocaloric effect in multiferroic Y-type hexaferrite Ba0.5Sr1.5Zn2(Fe0.92Al0.08)12O22. AIP Advances, 2014, 4, .	1.3	15
76	Fabrication and Dielectric Properties of <scp><scp>Ba</scp></scp> _{0.63} <scp><scp>Sr</scp>_{0.37}<scp>TiO</scp> Thin Films on <scp><scp>SiC</scp> Substrates. Journal of the American Ceramic Society, 2014, 97, 3048-3051.</scp></scp>	• <s 3.8</s 	ub>3
77	Marigold-like Cu x (x = 1.81 , 2) S \$mbox{Cu}_{x (x=1.81, 2)}mbox{S}\$ nanocrystals: controllable synthesis, field emission, and photocatalytic properties. Applied Physics A: Materials Science and Processing, 2014, 115, 801-808.	2.3	6
78	Structure and magnetic properties of La0.67Sr0.33MnO3 thin films prepared by sol–gel method. Journal of Sol-Gel Science and Technology, 2013, 67, 170-174.	2.4	15
79	Oxygen vacancy induced photoluminescence and ferromagnetism in SrTiO3 thin films by molecular beam epitaxy. Journal of Applied Physics, 2013, 114, .	2.5	31
80	The Cr-substitution concentration dependence of the structural, electric and magnetic behaviors for Aurivillius Bi5Ti3FeO15 multiferroic ceramics. Journal of Applied Physics, 2013, 114, .	2.5	41
81	The curing retardation and mechanism of high temperature vulcanizing silicone rubber filled with superconductive carbon blacks. Polymer Engineering and Science, 2011, 51, 170-178.	3.1	9
82	Emission mechanism in the terbium complex doped PVK system. Frontiers of Optoelectronics in China, 2008, 1, 130-133.	0.2	1